SCIENCE AT THE ENVIRONMENTAL RESEARCH STATION SCHNEEFERNERHAUS/ ZUGSPITZE

Prof. Dr. Michael Bittner; Ed.
(Coordinator Science Team UFS)
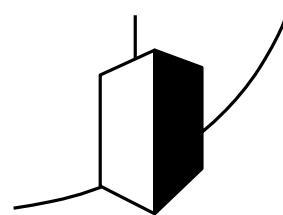
Umwelt
Forschungsstation
Schneefernerhaus

Table of contents

7 Temperature and Precipitation Anomalies at Mount Zugspitze in Relation to Large-scale Atmospheric Circulation Patterns and North-Atlantic European Modes of Variability

Jucundus Jacobeit and Markus Homann
Institute of Geography, University of Augsburg

Abstract

Relationships between the large-scale atmospheric circulation at the 500 hPa level and anomalies of temperature and precipitation at Mount Zugspitze are studied on monthly to seasonal time scales for the 1950–2015 period by two different approaches which are described in an extended methods section: firstly, T-mode principal component analysis (PCA) is used to determine basic circulation patterns during warm and cold months (winter, summer) and during wet and dry months (spring, autumn). Besides patterns with clear-cut association to one of these anomalies, other patterns exist with no distinct preference pointing to substantial internal variabilities (e. g. due to varying wave amplitudes and axis positions). Secondly, S-mode PCA derived modes of variability operating in context of teleconnection patterns like NAO (North Atlantic Oscillation), EA (East Atlantic Pattern), EAWR (East Atlantic West Russia Pattern) and SCAND (Scandinavian Pattern) are analyzed with respect to temperature or precipitation signals at Mount Zugspitze for pronounced positive and negative phases of these patterns. EA and EAWR turned out to show most often significant influence on seasonal climate anomalies at Mount Zugspitze.

Keywords: Mount Zugspitze, temperature, precipitation, circulation patterns, modes of variability, PCA, T-mode, S-mode

7.1 Introduction

Climate variability is closely linked to variations in the atmospheric circulation, and this relationship includes impacts from the large-scale dynamics of the atmosphere down to regional or even local climate conditions. In the present contribution, we will not use extended climate data sets for the whole Alpine region (Auer et al. 2007), but focus on Mount Zugspitze and its basic variables temperature and precipitation. Links to the large-scale atmospheric circulation are not analyzed with respect to weather types on a daily scale, but derived on climatic time scales (monthly to seasonal). This will be done not in terms of transfer functions in a classical downscaling context, but by means of two different approaches:

- at first basic circulation patterns (referring to the mid-tropospheric 500 hPa level) will be determined for those months with substantial deviations in temperature or precipitation from long-term mean conditions; these anomalies are defined by departures of more than one standard deviation above or below the corresponding mean values (cp. Jacobeit et al. 1998, p. 65).

- Secondly, we look at large-scale modes of variability (500 hPa level) in the North-Atlantic European area operating in context of particular teleconnection patterns according to the NOAA Climate Prediction Center (CPC). The most important ones – with respect to the target location – will be considered: North Atlantic Oscillation (NAO), East Atlantic Pattern (EA), East Atlantic West Russia Pattern (EAWR), and Scandinavian Pattern (SCAND). Since complete correlations with temperature or precipitation time series mostly do not yield convincing amounts of explained variance (see section 4.2), we focus on those months with pronounced anomalies in the time coefficients of these modes of variability (more than one standard deviation above or below the corresponding mean values) and analyze the associated temperature or precipitation signals at Mount Zugspitze.

Circulation patterns and modes of variability have to be determined by different variants of a powerful multivariate technique which will be explained and discussed in a separate section on basic approaches (section 3) before providing results with respect to the target location Mount Zugspitze (section 4).

7.2　Data

Daily temperature and precipitation time series are taken from the DWD (German Weather Service) measuring station Zugspitze, they are used for this contribution during the 1950–2015 period. This corresponds to the period of better quality in re-analysis data (NCAR/NCEP in this case, see Kalnay et al. 1996) from which the gridded geopotential height data (2.5° horizontal resolution) of the 500 hPa level have been extracted. Monthly time coefficients of the mid-tropospheric teleconnection patterns (NAO, EA, EAWR, SCAND) are taken from CPC's web site.

7.3　EOF/PCA techniques and their different modes of analysis

7.3.1　Some fundamentals

Before specifying the particular differences in analyzing data sets for circulation patterns or modes of variability, the general fundamentals of the underlying techniques should be elaborated. We try to give a condensed overview of what is explained in detail for example in the textbook of Jolliffe (2002). The principle aim of these techniques consists in replacing a large set of original variables V_i ($i = 1, …, n$) given for a certain number of cases k by a set of new quantities Q_j ($j = 1, …, m$) for the same cases k in such a way that their relation is described by the following set of equations

$$V_i = \sum_{j=1}^{m} l_{ij} \cdot Q_j + R_j \tag{1}$$

with $m \leq n$, l_{ij} as so-called *loadings* which constitute the linear combinations for V_i, and R_i as the remaining residuals in the set of equations. This transformation will be effective if the number of new quantities Q is considerably lower than the number of original variables V and if, at the same time, the residuals remain as small as possible: this would maintain the largest amount of information and allow a simplified representation which not only reduces the dimensionality of the data set, but also condenses the information to basic quantities with noise being filtered out. If Q_j are determined in context of empirical orthogonal function (EOF) or principal component analysis (PCA), they are even orthogonal (uncorrelated) to each other and constitute linear combinations for V_i by mutually independent basic quantities. The loadings provide the varying weights of these basic quantities in composing the different original variables.

As a first step for deriving these loadings, a correlation or a covariance matrix C is calculated from the original variables quantifying the degree of relationship for all pairs V_i, V_j ($i, j = 1, …, n$). Correlation coefficients reflect standardized relationships without physical units whereas the latter are maintained in case of calculating covariances. From matrix C a characteristic polynomial is generated by the determinant

$$\det(C - \lambda \cdot U), \text{ (}U\text{: unit matrix)}$$

whose zero positions λ_j ($j = 1, …, m$) are called Eigen-values. They allow to calculate orthogonal Eigen-vectors EV_j by means of the linear equation system

$$(C - \lambda_j \cdot U) \cdot EV_j = 0$$

The components ev_{ij} of Eigen-vector EV_j ($i = 1, …, n$) correspond to the loadings l_{ij} in EOF analysis, whereas in PCA the loadings are given by

$$l_{ij} = \sqrt{\lambda_j} \cdot ev_{ij}$$

Weighting the Eigen-vector components by the square root of the corresponding Eigen-value implies that these PCA loadings represent the correlation coefficients between the original variables V_i and the principal components PC_j (as far as C has been calculated as correlation matrix). They indicate the degree of relationship for all pairs of V_i and PC_j and thus allow to interpret the PCs in terms of properties characterizing sub-groups of variables with higher loadings on the same PCs.

Since squared correlation coefficients provide explained variances between the correlated quantities, statements on V_i and PC_j in terms of explained variances are possible by means of squared loadings l_{ij}^2: summing them up for a particular PC_j for $i = 1, ..., n$ – this gives the Eigen-value λ_j – and dividing it by the number of variables n, provides the amount of total variance in the data set explained by PC_j indicating its relative importance among all PCs in composing the original variables according to the set of equations (1). These explained variances λ_j/n decrease from $j = 1$ to $j = m$, since the Eigen-values λ_j constitute a descending sequence. Summing up the squared loadings for a particular variable V_i for $j = 1, ..., m$ yields the so-called communalities indicating to which degree V_i is represented by all the included PCs (on the decision of their number m see later on).

Besides the loadings l_{ij}, EOF and PC analyses provide a second part of results, the so-called *scores* (or sometimes *amplitudes*) giving the values of the new quantities Q for all cases k covered by the original variables V. They can directly be calculated as

$$Q = (L^T \cdot L)^{-1} \cdot L^T \cdot V$$

with L as loadings matrix and L^T as its transposed variant (exchange between rows and columns). Thus, the scores specify the behavior of the EOFs or PCs across all cases k, whereas the loadings indicate their relationships to the original variables V.

It should be mentioned that the term "principal components" is sometimes used in another way (especially in Meteorology and Climate Research) reducing it to what we have called scores (or amplitudes), whereas in our context PCs include both parts of results (loadings as well as scores) motivated by the fact that these analyses can be run in different modes with different meanings of loadings and scores (see 3.2).

If C has been calculated as covariance matrix, one part of the results maintains the physical units (the other part being dimensionless). If the units shall be linked with the loadings l_{ij}, the operation mode PCA is necessary (i. e. weighting Eigen-vector components by the square root of the corresponding Eigen-value) with scores being divided by this λ square root (von Storch and Zwiers 1999).

In many cases EOFs or PCs are rotated in such a way that the assignment of original variables to EOFs or PCs is optimized. Rotation is especially reasonable if EOFs or PCs represent different regional domains, whereas no rotation should be applied if the focus is only on some few of the leading modes. As a result of rotation, explained variances are re-distributed among the EOFs or PCs with decreasing amounts for the leading ones and increasing amounts for the subordinated ones. Rotation can be done in different ways: maintaining orthogonality between the EOFs or PCs, but also running oblique rotations with PCs being no longer uncorrelated and the loadings l_{ij} being no longer identical with the correlations/covariances between V_i and PC_j.

A crucial point is the decision for an appropriate number of EOFs or PCs influencing the results especially if rotation is applied. There is a lot of criteria starting from simple ones (extracting only EOFs or PCs with $\lambda \geq 1$ according to *Kaiser* or using particular minimum thresholds for (individual or total) explained variances) to standard ones (like the 'elbow criterion' looking for distinct jumps in the sequence of Eigen-values) to more sophisticated ones (e. g. extracting only EOFs or PCs whose time coefficients significantly differ from white noise). Quite often some kind of a dominance criterion (Jacobeit 1993) can effectively be used considering only those EOFs or PCs which dominate at least one input variable (in terms of above-average (by more than one standard deviation) rotated loadings with respect to those of all other variables and EOFs/PCs, respectively). Thus, meaningless candidates which do not reflect real conditions but only represent background noise will not be extracted. For distinctly complex data sets, a further extension of this dominance criterion might be necessary, e. g. with respect to significant field correlations between input variables and EOF/PC scores (Philipp et al. 2007). Finally, be-

yond any statistical criteria, it might be reasonable to use only those EOFs/PCs which can be seen as manifestations of real processes or conditions and can be interpreted in a sound scientific manner.

It should additionally be mentioned that EOF and PC analyses can also be applied to a set of temporal sequences of spatial fields (extended analysis or principal sequence pattern analysis, see Compagnucci et al. 2001, Jacobeit et al. 2006) as well as to several fields (combined analysis) referring for example to different atmospheric levels or to different wind components (e. g. Jacobeit 1992). Furthermore, coupled pairs of patterns from two fields of related variables can be derived by canonical correlation analysis (CCA, e. g. Dünkeloh and Jacobeit 2003), and principal oscillation pattern (POP) analysis refers to patterns evolving in time (e. g. Schnur et al. 1993).

7.3.2 Different modes of analysis

Richman (1986) has made a distinction into six different modes of EOF/PC analysis depending on what kind of quantities is processed as input variables and on the nature of the cases for which values of these variables are included. Table 1 summarizes these six modes which imply different meanings of loadings and scores, respectively:

Tab. 1: Different modes of EOF/PC analysis in Meteorology and Climate Research (according to Richman 1986) defined by different settings of variables and cases

Mode	variables	cases
R-mode	meteorological parameters	spatial units
P-mode	meteorological parameters	temporal units
Q-mode	spatial units	met. parameters
O-mode	temporal units	met. parameters
S-mode	spatial units	temporal units
T-mode	temporal units	spatial units

- With R-mode (in our context meteorological parameters as variables, spatial units like stations or grid points as cases) the scores yield spatial patterns and the loadings reveal their meteorological meaning.
- With P-mode (once more meteorological parameters as variables, but now temporal units (days or months or years …) as cases) the scores yield characteristic time series whose meteorological meaning is revealed by the loadings.
- With Q-mode (spatial units as variables, meteorological parameters as cases) a spatial composition (with spatial coherence even a regionalization) in terms of a set of characterizing parameters is achieved.
- With O-mode (temporal units as variables, meteorological parameters as cases) a temporal distinction in terms of a set of characterizing parameters is achieved.
- With S-mode (spatial units as variables, temporal units as cases) the loadings provide spatial patterns and the scores their time coefficients with respect to the included parameters (e. g. air pressure or temperature or precipitation …).
- With T-mode (temporal units as variables, spatial units as cases) the scores provide spatial patterns and the loadings their time coefficients with respect to the included parameters.

In Meteorology and Climate Research, mostly S- and T-modes (including both spatial and temporal resolutions) are applied, and they directly lead to our objectives, modes of variability and basic circulation patterns, respectively. Starting with the latter, the fundamental idea consists in generating some few patterns which represent basic states of the atmospheric circulation in the study domain (e. g. a zonal pattern, a trough-like pattern, a ridge-like pattern etc.) from which all original fields (SLP or geopotential height fields for a number of temporal units like days or months) can be reproduced by linear combinations with varying time coefficients. The latter correspond to the T-mode loadings which specify the particular weight of the basic patterns (given by the T-mode scores) within the original fields reflecting their degree of similarity to the

7

basic patterns (Jacobeit et al. 2001). For example, a westerly flow at a particular date would have a dominant loading on a basic zonal circulation pattern. Thus, each individual field can be characterized by dominating and receding basic patterns allowing to group the original fields according to their different affinity to the basic patterns.

It has to be stressed that this procedure is not an usual classification since the attribution of original fields to basic patterns is not an unequivocal one (like in disjunctive classifications where each variable belongs to one and only one of the classified types). The EOF/PC loadings, however, also include non-zero values for those patterns which are not the leading ones thereby accounting for the fact that most variables contain elements from more than one basic pattern. Therefore, the correct view of (squared) loadings is a representation of varying amounts of explained variance with increasing and decreasing values for a particular pattern from one variable to the next. Comparing these values among all basic patterns allows to characterize the atmospheric circulation of the original fields with respect to these basic patterns. In T-mode, they have furthermore to be distinguished from centroid patterns resulting from classifications of circulation types: the latter result from averaging all the individual members of a classified type, whereas the T-mode scores are not averaged from individual objects, they represent a generic circulation pattern (Jacobeit 2010), some kind of a prototype with varying degrees of similarity to the original fields (expressed by the T-mode loadings). Thus, the individual objects are reproduced as superimpositions of prototype patterns with varying weights according to equation (1), and these prototype patterns reflect basic states of the atmospheric circulation as far as they prove to be no artefacts but manifestations of well-known patterns from the real dynamical system.

The other approach linked with S-mode circulation analyses intends to identify characteristic time series of SLP or geopotential height data being representative for a certain number of grid-points in the study domain (Jacobeit et al. 1998, p. 55). Therefore, these grid-points define the input variables which are replaced by EOFs/PCs constituting spatial centres of variation with corresponding S-mode scores providing these characteristic time series. The S-mode loadings reflect the degree of similarity between these scores and the original grid-point time series. High loadings indicate such a centre of variation which is characterized by a particular mode of temporal variability in SLP or geopotential heights. If the study domain is large enough, further loading maxima (positive or negative) may occur outside the primary centre of variation; in this case the field of loadings even provides teleconnection patterns indicating which regions are connected to each other in terms of same or opposite directions in temporal variability. For example, in the North-Atlantic European area the first winter-time S-mode EOF/PC mostly reflects the North-Atlantic Oscillation (NAO) with opposite loadings in the regions around Iceland and the Azores (other teleconnection patterns will be addressed in the next section). However, S-mode loading patterns cannot be interpreted as circulation patterns (like T-mode scores), since the maxima and minima do not represent high and low pressure centres, but locations with highest similarity (positive or negative) to the corresponding mode of temporal variability. Thus, in S-mode, scores describe the varying phases of teleconnections whose spatial patterns are specified by the loadings.

Summing up, S- and T-modes not only differ in the attributes of loadings and scores – the former giving spatial (temporal) information, the latter temporal (spatial) information in S-(T-)mode – but also in the meaning with respect to atmospheric circulation dynamics (see also Compagnucci and Richman 2008). S-mode analysis provides teleconnection patterns (if we focus on the spatial dimension) or modes of variability (if we focus on the temporal dimension), whereas T-mode analysis provides basic circulation patterns into which original fields can be decomposed. Especially the T-mode scores have great importance as generic circulation patterns whose superimpositions with varying weights reproduce the original fields and condense their information to a few decisive patterns. If we combine both modes of analysis, a comprehensive picture of atmospheric circulation dynamics can be initiated.

7.4 Results with respect to Mount Zugspitze

In this section we focus on relationships between the atmospheric circulation and both temperature and precipitation anomalies at Mount Zugspitze, and this will be done by using basic circulation patterns (derived from T-mode PCA, section 4.1) as well as modes of variability/teleconnection patterns (based on S-mode PCA, section 4.2).

7.4.1 Atmospheric circulation patterns

To identify relationships between temperature or precipitation and basic circulation patterns, we focus (as input variables for T-mode analysis) only on those months which differ (with positive or negative sign) by more than one standard deviation from the corresponding long-term mean value thus excluding all months near to average climate conditions. Based on these substantial anomalies which in most cases amount to seasonal numbers between 55 and 71 for the 1950–2015 period (only for wet and dry winter months a lower number of 44 is reached), distinct signals in the large-scale mid-tropospheric circulation (500 hPa level) can be expected.

From the eight analyses (temperature and precipitation anomalies separately for the meteorological seasons) we select in this chapter those referring to warm and cold anomalies during winter and summer as well as wet and dry anomalies during spring and autumn. The remaining analyses include some overlapping results and therefore can be left out.

7.4.1.1 Warm and cold anomalies during winter (DJF)

During the 1950–2015 period, 36 warm (more than one standard deviation above the long-term mean value) and 35 cold months (more than one standard deviation below the long-term mean value) occurred at Mount Zugspitze. With the monthly mean geopotential height fields (500 hPa level) of these 71 months as input variables, we get four (according to the dominance criterion) rotated T-mode principal components each explaining more than 10 % of the original variance (all together nearly 97 %). Fig. 1 displays the corresponding basic circulation patterns (T-mode scores), Fig. 2 is based on the time coefficients (T-mode loadings) indicating in squared terms the variances explained by each PC split up into warm and cold months. If there is a significant difference between these sub-samples (95 % level according to Mann-Whitney's U-test), the corresponding circulation pattern is associated either to warm or to cold anomalies, the above-average value in Fig. 2 being averaged from those months with dominance of the corresponding PC (greatest loading among all PCs). If there is no significant loading difference between warm and cold sub-samples, the corresponding circulation pattern proves as a mixed one with alternating predominance during both thermal anomalies.
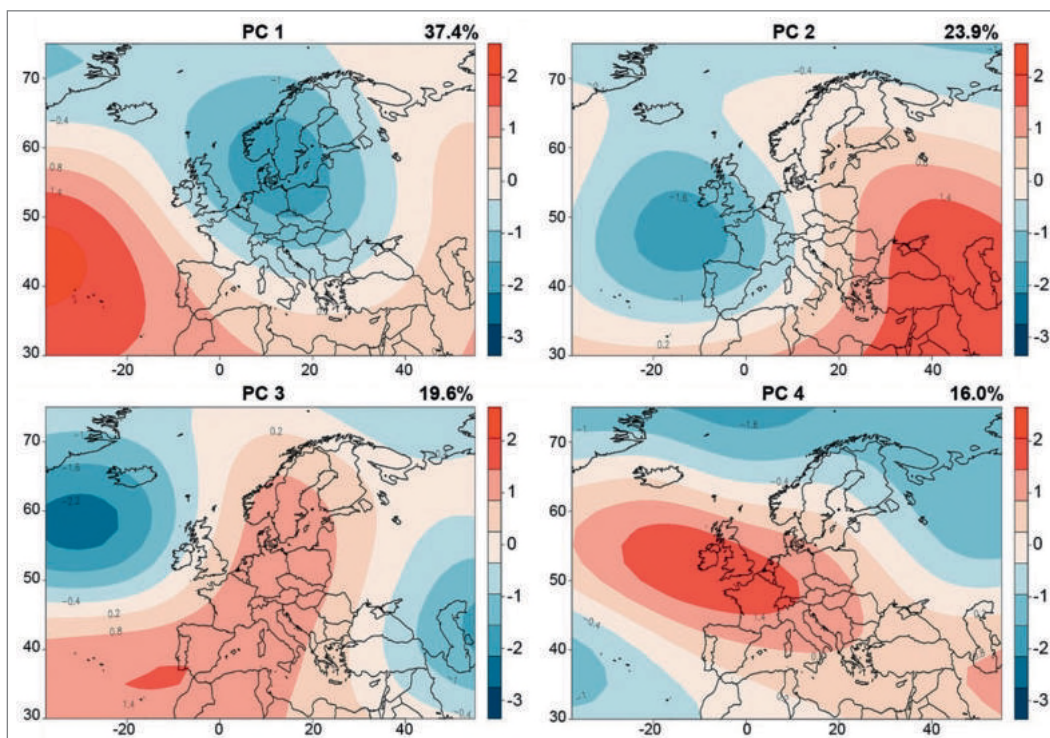
Fig. 1: Basic circulation patterns for warm and cold months (more than one standard deviation above or below the corresponding mean values) at Mount Zugspitze during winter (DJF) 1950–2015 derived from T-mode PCA of monthly mean geopotential height grids at the 500 hPa level (explained variances in %).
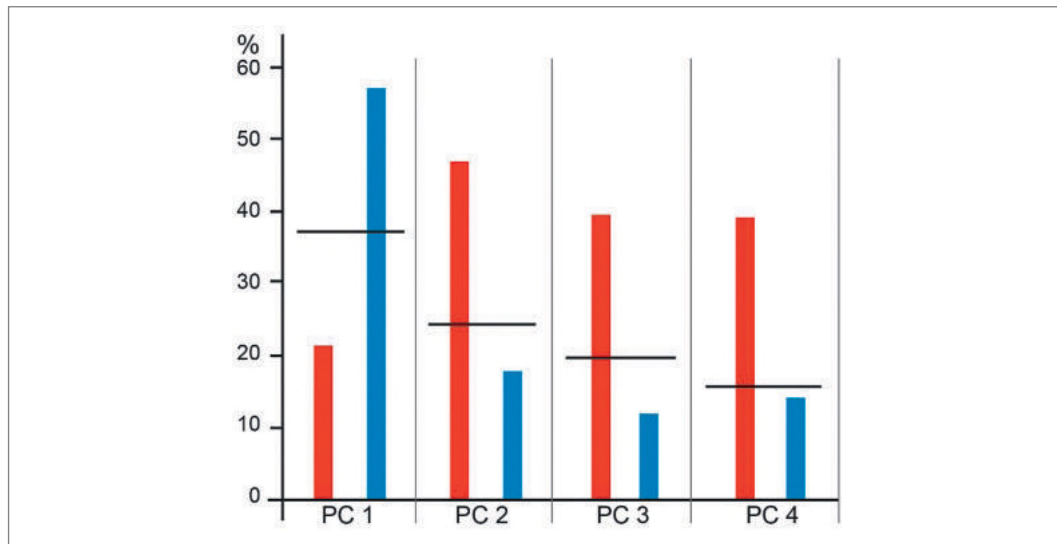
Fig. 2: Mean squared T-mode loadings (corresponding to explained variances in %) of PCs 1–4 from the geopotential height analysis for warm and cold months (red and blue color, respectively) during winter (DJF) 1950–2015. Black lines represent the mean values for each PC, red and blue values above this reference are averaged from those months with dominance of the corresponding PC (greatest loading among all PCs), red and blue values below this reference are averaged from all warm or cold winter months indicating systematic loading differences between them.

PC 1 clearly prevails during cold winter months, it represents a trough pattern with the cyclonic centre above southern Scandinavia and Mount Zugspitze at the rear of the cyclonic wave where (sub-)polar cold air is advected towards lower latitudes. This well-known pattern for strong winter conditions in large parts of the western and central European mid-latitudes (e.g. Jacobeit et al. 1998, p.125) even accounts for nearly all cold winter months at Mount Zugspitze. Since it is linked with northerly to north-westerly wind directions, one might ask for another well-known 'cold' pattern characterized by a strong and westward extended Russian high with easterly components in Central Europe (Jacobeit et al. 2009, p. 41). Indeed, such patterns prevail (with varying high pressure positions) during nearly the half of all cold winter months, however, the Russian high as a thermal pressure system with only limited vertical extension merely is present at lower atmospheric levels and cannot be identified any more at 500 hPa. Thus, PC 1 remains as the only mid-tropospheric pattern with a distinct linkage to cold winter months.

The other three circulation patterns of Fig. 1 are primarily related to warm winter months (see Fig. 2) and therefore might gain increased importance with enhanced global warming. PC 2 represents a pattern dominated by a low pressure system above the mid-latitudinal eastern Atlantic (high pressure only further to the east) with the Zugspitze region in front of it being located in the large-scale flow from southerly to south-westerly directions. PC 3 looks like a PC-2 pattern shifted towards the north-west, thus the Zugspitze region is included into the warm core of the anticyclonic ridge above continental Europe. The PC-4 pattern – already with insignificant loading differences, but mainly dominating during warm months – still displays another high-pressure centre now extending more in a zonal direction. Altogether, warm winter months are linked either to warm cores of meridional or zonal high pressure ridges or to wave patterns with warm air advection between the cyclonic phase to the west and the anticyclonic one to the east (PC 2).

It should furthermore be mentioned that particular shifts within the patterns of Fig. 1 are able to lead to opposite temperature effects: for example, if the wave pattern of PC 2 is shifted sufficiently to the east, the Zugspitze region might get into the cold core of the cyclonic wave (as in three cases of cold winter months). Another within-pattern change can take place if the high-pressure centre of PC 4 is sufficiently shifted to the west so that the Zugspitze region in front of it gets into the cold north-westerly flow (one case during the study period). Apart from these internal changes, however, the basic circulation patterns of Fig. 1 have a clear preponderance to either warm or cold anomalies during winter time.

7.4.1.2 Warm and cold anomalies during summer (JJA)

During the 1950–2015 period, 38 warm and 27 cold months occurred at Mount Zugspitze. Submitting the monthly mean geopotential height fields (500 hPa level) of these 65 months to a rotated T-mode PCA results in four PCs each explaining more than 20 % of the original variance (all together more than 96 %). Like in the preceding section, Figs. 3 and 4 reproduce the basic circulation patterns and their differences between warm and cold months.

According to Fig. 4, PC 1 is clearly linked to warm summer months, the corresponding circulation pattern (Fig. 3) is well-known from other studies (e. g. Jacobeit et al. 2003) and represents an anticyclonic ridge from the Azores region towards southern Scandinavia with the Zugspitze region being included in the warm core of this ridge. In contrast to that, PC 2 shows a trough pattern in this longitudinal section, high pressure influence is located upstream above the central North Atlantic. Accordingly, the Zugspitze region is exposed to cold advection from northerly to north-westerly directions, PC 2 proves to be a cold-anomaly pattern.

The remaining two PCs do not have a significant relationship to a particular temperature anomaly at Mount Zugspitze, warm as well as cold summer months may occur with them (Fig. 4).
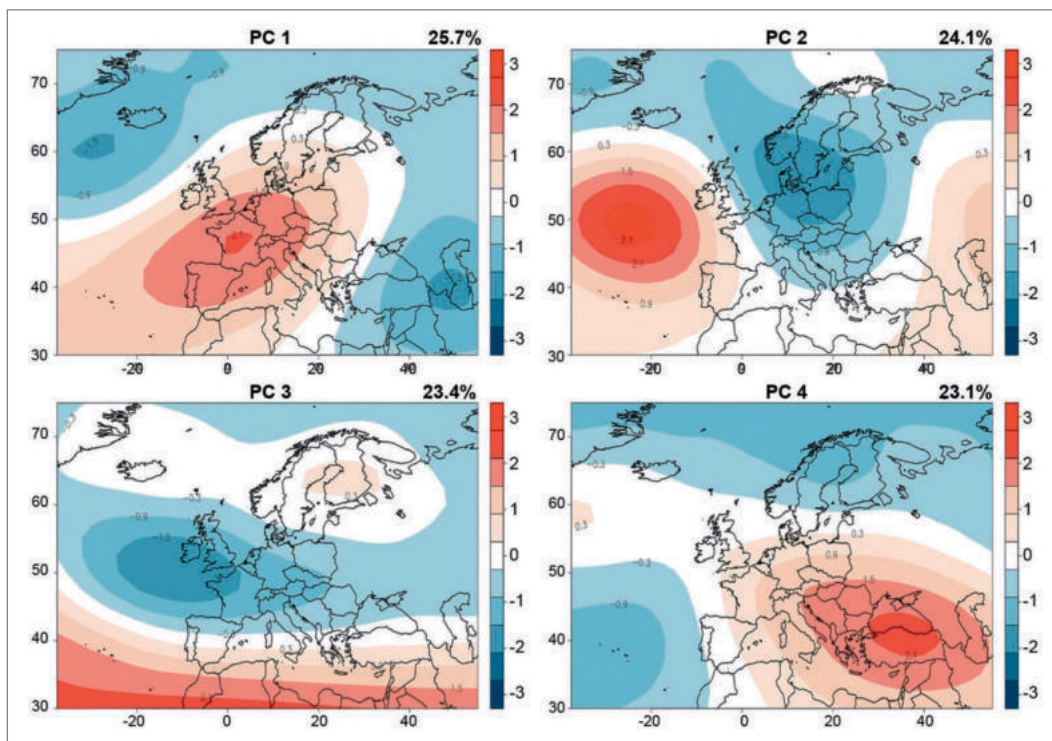
Fig. 3: As Fig. 1 but for warm and cold months during summer (JJA)
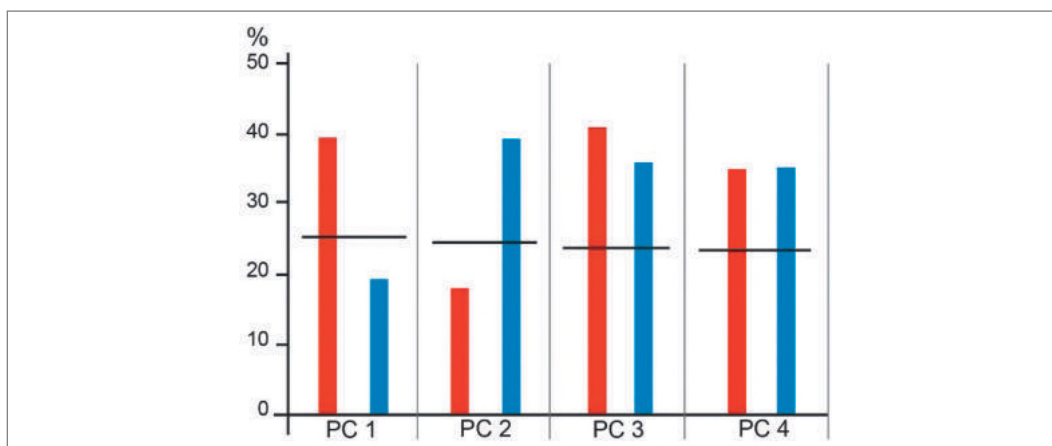
Fig. 4: As Fig. 2 but for warm and cold months during summer (JJA)
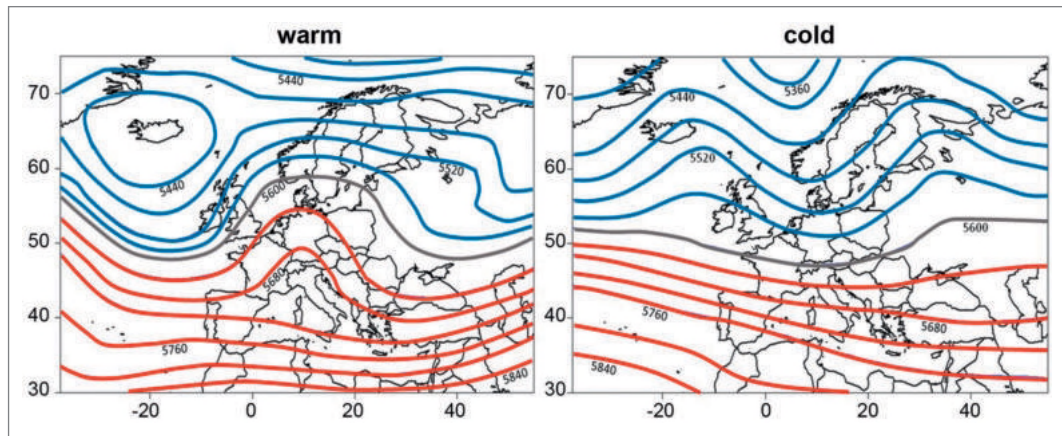
Fig. 5: Composites of monthly mean 500 hPa geopotential heights (gpm) for those warm or cold summer months having the highest loading on PC 3 from Fig. 3
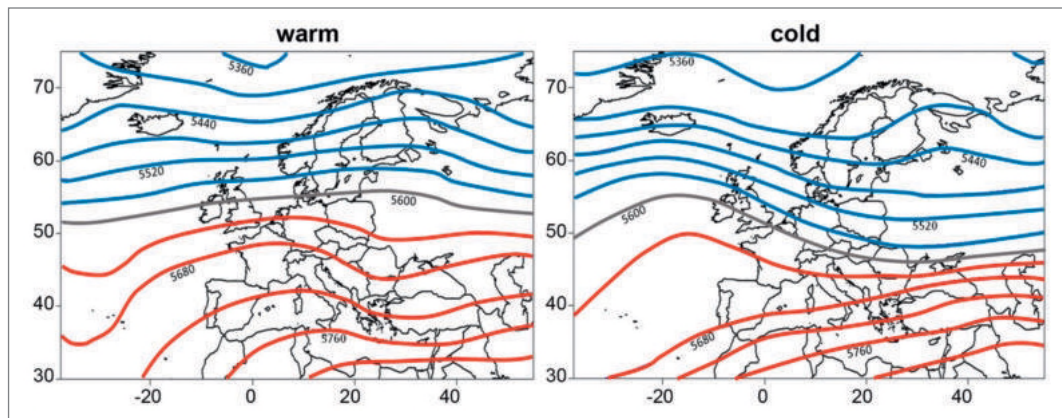
Fig. 6: As Fig. 5 but for PC 4 from Fig. 3

PC 3 depicts a cyclonic centre towards the west, PC 4 an anticyclonic one towards the south-east. Figs. 5 and 6 reveal the background of their thermal ambiguity: comparing the PC composites for the opposite thermal anomalies (i.e. the loading-weighted mean geopotential height fields for all warm or cold months linked to a particular PC) indicates in case of PC 3 that the cyclonic phase of the wave pattern is located considerably further west (further east) during warm (cold) summer months. In case of PC 4, an anticyclonic wave is developed around the Zugspitze region during warm months instead of north-westerly components during cold months. Thus, internal variations within these PC patterns imply the occurrence of different temperature anomalies, depending for example on varying wave lengths and phase positions like for PC 3 and PC 4.

7.4.1.3 Wet and dry anomalies during spring (MAM)

During the 1950–2015 period, 29 wet and 32 dry months occurred at Mount Zugspitze. Submitting the monthly mean geopotential height fields (500 hPa level) of these 61 months to a rotated T-mode PCA results in four PCs each explaining more than 15 % of the original variance (all together 97 %). Like in the preceding sections, Figs. 7 and 8 reproduce the basic circulation patterns and their differences now between wet and dry months.

A clear link to wet (dry) conditions exists for PC 4 (PC 2) with the Zugspitze region in the core of a central low (high) pressure system. For PC 1 and PC 3, however, the circulation-precipitation link is ambiguous (Fig. 8) due to pressure centres located more westward with varying extensions towards the Zugspitze region. For the wet version of PC 1(see Fig. 9), the cyclonic wave amplitude reaches more than 5° of latitude further south than for the dry version of the same PC. For PC 3 (see Fig. 10), the position of the anticyclonic wave axis differs by some 10° of longitude between wet and dry conditions, and this is decisive whether or not the Zugspitze region is included in its spatial domain. Thus, once more internal variations within particular PC patterns may influence the sign of a local climate anomaly.
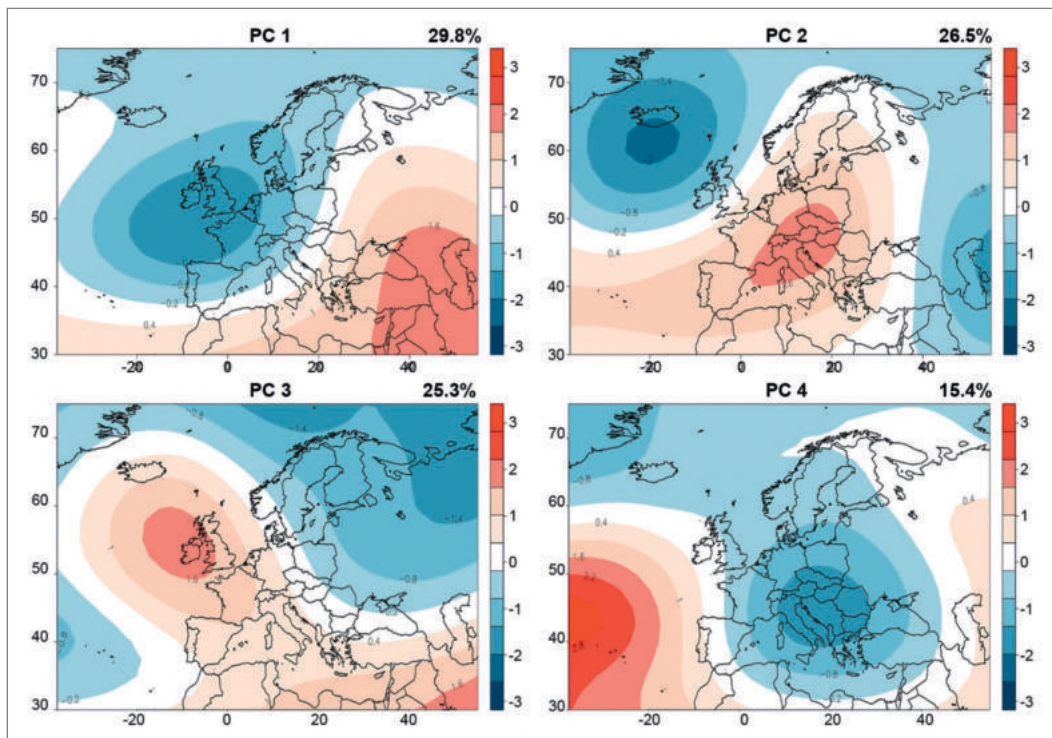
Fig. 7: As Fig. 1 but for wet and dry months during spring (MAM)
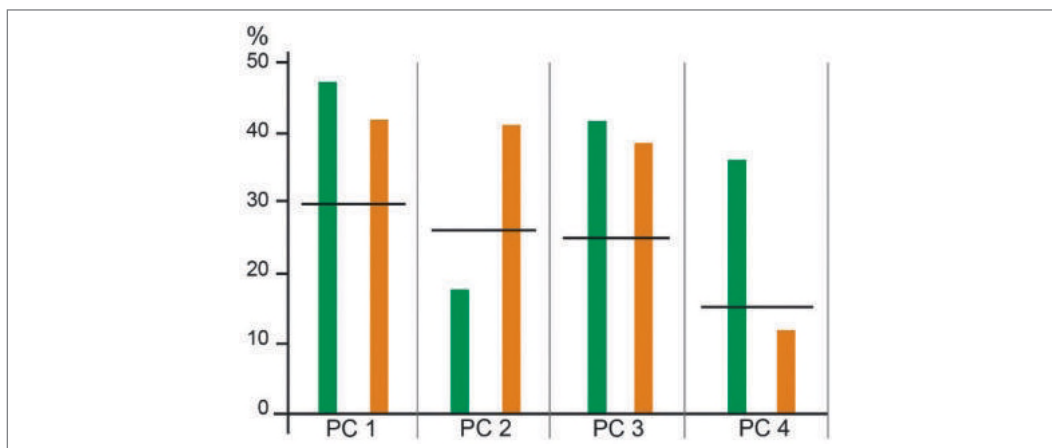
Fig. 8: As Fig. 2 but for wet and dry months (green and brown color, respectively) during spring (MAM)

7.4.1.4 Wet and dry anomalies during autumn (SON)

During the 1950–2015 period, 25 wet and 30 dry months occurred at Mount Zugspitze. Submitting the monthly mean geopotential height fields (500 hPa level) of these 55 months to a rotated T-mode PCA results in four PCs each explaining more than nearly 10 % of the original variance (all together 97 %). Like in the preceding section, Figs. 11 and 12 reproduce the basic circulation patterns and their differences between wet and dry months.

PC 1 represents an anticyclonic ridge pattern from the Azores towards central Europe and is clearly linked to dry autumn months at Mount Zugspitze. Most of the wet months are related to PC 2 representing a central European trough pattern. The remaining PCs show some similarity to spring patterns and therefore are not specified by further composites: PC 3 generally resembles the first spring pattern concerning the wave phase positions and may likewise be linked to both wet and dry autumn months depending on varying amplitudes of the cyclonic wave to the west of Mount Zugspitze. Similar internal variations as for spring pattern 3 apply to PC 4 which, however, is realized in autumn 1950–2015 only in the dry version concerning Mount Zugspitze; therefore, no above-average value occurs for 'wet' in Fig. 12, but the loading difference between wet and dry remains insignificant.
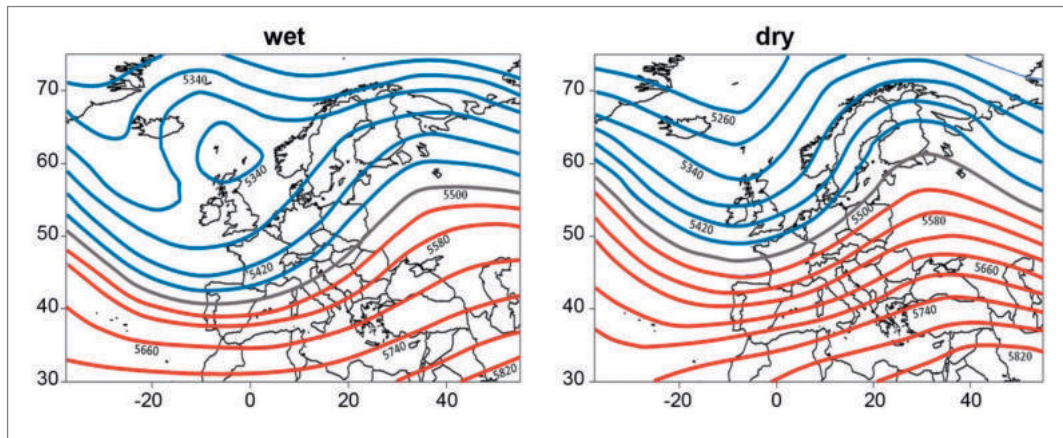
Fig. 9: Composites of monthly mean 500 hPa geopotential heights (gpm) for those wet or dry spring months having the highest loading on PC 1 from Fig. 7
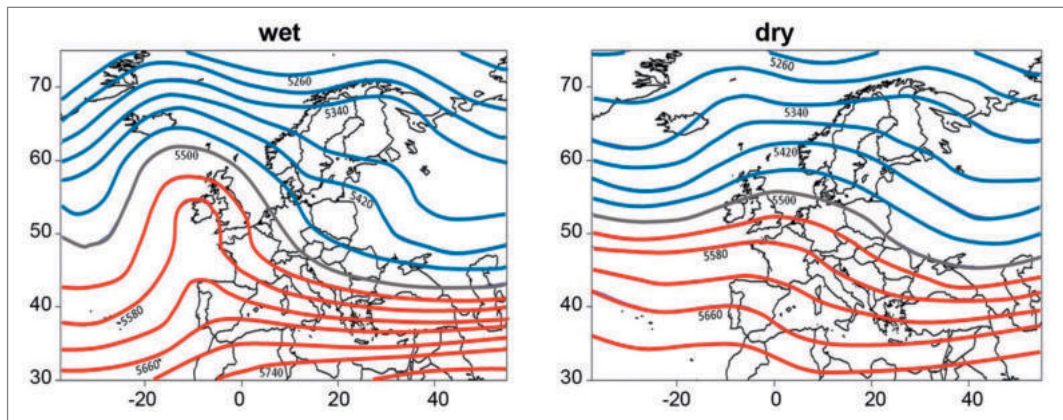
Fig. 10: As Fig. 9 but for PC 3 from Fig. 7
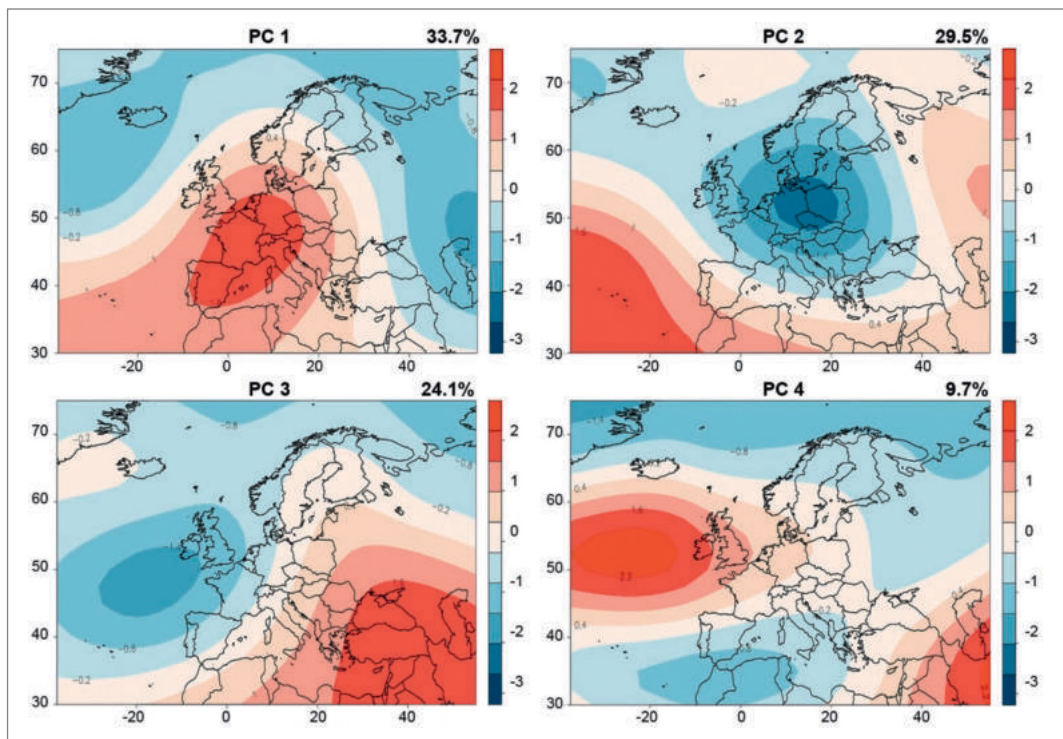
Fig. 11: As Fig. 1 but for wet and dry months during autumn (SON)
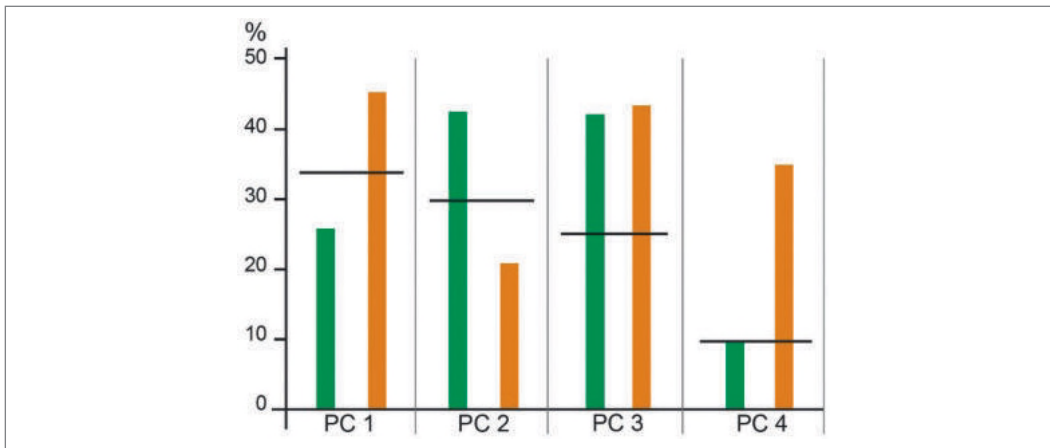
Fig. 12: As Fig. 8 but for wet and dry months during autumn (SON)
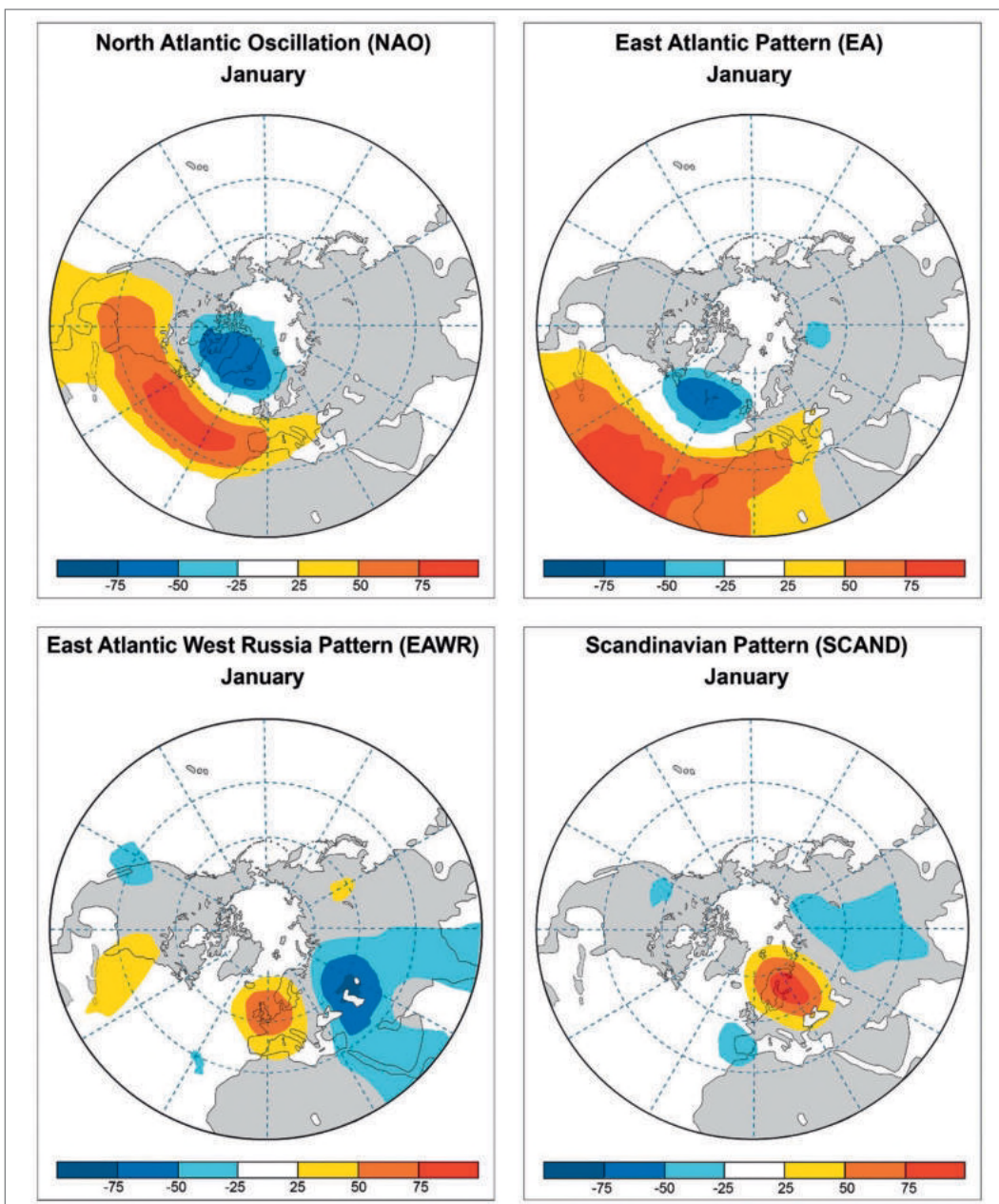
Fig. 13: The S-mode loading patterns for NAO, EA, EAWR and SCAND for the selected month of January in terms of the temporal correlation coefficients between the monthly normalized geopotential height anomalies (500 hPa level) at each grid point and the S-mode score time series for the corresponding tele-connection patterns (modified after Climate Prediction Center CPC).

7.4.2 Modes of variability / teleconnection patterns

In contrast to basic circulation patterns discussed in the previous sections, we now focus on possible impacts of large-scale modes of variability (referring again to the 500 hPa level) on monthly temperature and precipitation conditions at Mount Zugspitze. These modes of variability are provided by characteristic time series of well-known teleconnection patterns derived by S-mode EOF/PC analysis. In our context we focus on the most important teleconnection patterns in the North-Atlantic European region (NAO, EA, EAWR, SCAND, see Fig. 13) using their monthly time coefficients 1950–2015 as provided by the Climate Prediction Center (CPC).

Direct correlations between these time coefficients and the Zugspitze temperature or precipitation time series mostly yield small absolute values (lower than 0.4 corresponding to explained variances of distinctly less than 20 %), only for the EA pattern and Zugspitze temperature there are slightly higher values (with maxima of 0.52 and 0.51 for autumn and winter, respectively). Considering time lags – as might be reasonable in teleconnective relationships – does not increase the correlation coefficients, they further drop down to even smaller values (maximum 0.21), probably arising from the monthly time scale of these analyses. In view of that, we prefer another 'anomaly approach', focusing on those months with deviations in the time coefficients for the teleconnection patterns of more than one standard deviation above or below the long-term mean values. For these anomaly months, the associated seasonal temperature and precipitation signals at Mount Zugspitze are quantified in two different ways: at first, providing the percentage frequencies of positive and negative deviations in temperature and precipitation for both anomaly phases of the teleconnection patterns; secondly, specifying for these opposite teleconnection phases the mean values of normalized temperature and precipitation, separately for positive and negative deviations. Thereby, possible impacts of pronounced teleconnection pattern anomalies on temperature and precipitation conditions at Mount Zugspitze will be identified on a seasonal basis.

7.4.2.1 North Atlantic Oscillation (NAO)

The well-known impacts of the NAO on the European climate (e. g. Appenzeller et al. 2000) are confirmed for the Zugspitze region (Tab. 2): the strongest signal (significant at the 99 % level according to a two-tailed χ^2-test) can be achieved for winter temperature with 75 % (59 %) of the pronounced NAO+ (NAO-) cases showing positive (negative) deviations at Mount Zugspitze with normalized mean values of +0.91 (-1.10). The same relationship – higher temperatures with strong mid-latitude westerlies and lower temperatures with decreased westerlies or more meridional circulation patterns – can still be seen for autumn though less pronounced (Tab. 2). During spring and summer, significance cannot be reached any more. Similar seasonal differences exist for precipitation with one important exception, however: NAO+ during autumn tends to be accompanied with below-average precipitation (75 % of all cases) in contrast to winter with the majority (67 %) pointing to above-average precipitation. This opposition is based on the fact that during the warmer half of the year the NAO+ does not represent a westerly but rather an anticyclonic ridge pattern from the Azores towards southern Scandinavia in prolongation of the high-summer NAO according to Folland et al. (2009). Altogether, NAO- does not include distinct signals in monthly Zugspitze precipitation, whereas NAO+ often leads to more (less) precipitation in winter (autumn).

7.4.2.2 East Atlantic Pattern (EA)

This pattern is similar to a southward shifted NAO pattern (see Fig. 13), its major centre of variation (implying negative geopotential height anomalies in the positive phase EA+) is located in the eastern mid-latitude Atlantic (west of the British Isles). There is a highly significant (99 % level, see Tab. 3) temperature signal at Mount Zugspitze during all seasons with clearly dominating positive deviations during EA+ (with frequencies between 76 and 95 % and mean normalized anomalies mostly greater than 1) and prevailing negative deviations during EA- (with frequencies between 68 and 80 % and mean normalized anomalies near -1). In terms of circulation dynamics this is due to a large-scale south-westerly (north-westerly) flow in front of an eastern Atlantic low (high) pressure system.

The signals in Zugspitze precipitation are less distinct (Tab. 3) attaining significance only in summer (99 % level) and autumn (95 % level), and this is mainly due to EA+ with dominating

Tab. 2: Frequency (a) and intensity (b) of positive and negative deviations from the long-term mean in monthly temperature and precipitation at Mount Zugspitze for NAO+ and NAO- during the meteorological seasons (DJF, MAM, JJA, SON). Percentage frequencies refer to all months with deviations in the seasonal NAO time coefficient of more than one standard deviation above or below the long-term mean value. 2×2 sub-tables for a particular season and variable providing a significant two-tailed χ^2-test are highlighted in dark and light color for the 99% and 95% level, respectively. Intensity is indicated by the mean value of the normalized monthly temperature or precipitation anomalies during those months counted in the frequency table.

a)

Frequency	Temperature ↑	Temperature ↓	Precipitation ↑	Precipitation ↓
Winter NAO+	75%	25%	67%	33%
Winter NAO-	41%	59%	49%	51%
Spring NAO+	59%	41%	52%	48%
Spring NAO-	49%	51%	49%	51%
Summer NAO+	53%	47%	37%	63%
Summer NAO-	49%	51%	44%	56%
Autumn NAO+	65%	35%	25%	75%
Autumn NAO-	39%	61%	48%	52%

b)

Intensity	Temperature ↑	Temperature ↓	Precipitation ↑	Precipitation ↓
Winter NAO+	0.91	-0.53	0.64	-0.61
Winter NAO-	0.64	-1.1	0.24	-0.56
Spring NAO+	0.79	-0.64	0.97	-0.59
Spring NAO-	0.71	-0.90	0.61	-0.66
Summer NAO+	0.65	-0.63	0.68	-0.77
Summer NAO-	0.89	-0.89	0.98	-0.58
Autumn NAO+	0.86	-0.79	1.05	-0.81
Autumn NAO-	0.85	-0.80	0.79	-0.58

Tab. 3: As Tab. 2 but for the East Atlantic Pattern (EA)

a)

Frequency	Temperature ↑	Temperature ↓	Precipitation ↑	Precipitation ↓
Winter EA+	81%	19%	59%	41%
Winter EA-	29%	71%	62%	38%
Spring EA+	76%	24%	41%	59%
Spring EA-	32%	68%	48%	52%
Summer EA+	83%	17%	22%	78%
Summer EA-	27%	73%	50%	50%
Autumn EA+	95%	5%	37%	63%
Autumn EA-	20%	80%	55%	45%

b)

Intensity	Temperature ↑	Temperature ↓	Precipitation ↑	Precipitation ↓
Winter EA+	1.01	-0.32	0.22	-1.03
Winter EA-	0.46	-0.96	0.82	-0.96
Spring EA+	0.89	-0.56	0.62	-0.57
Spring EA-	0.59	-1.07	1.15	-0.72
Summer EA+	1.28	-1.04	1.12	-0.58
Summer EA-	0.63	-0.84	0.69	-0.64
Autumn EA+	1.01	-0.61	0.35	-0.62
Autumn EA-	0.68	-1.04	0.92	-0.76

7

negative deviations in precipitation linked with the large-scale south-westerly flow. Otherwise, internal variations within the EA pattern concerning position and strength of the driving centre seem to prevent further significant signals in precipitation.

7.4.2.3 East Atlantic West Russia Pattern (EAWR)

This pattern includes two opposing centres of variation above Western Europe (centered around the North-Sea) and in the Caspian Sea region (Fig. 13). Its positive phase EAWR+ is defined for an anticyclonic system to the west and a cyclonic one further east. Temperature signals at Mount Zugspitze are highly significant (99 % level) for three seasons (Tab. 4), only in summer no clear distinction between the opposite EAWR phases is present. Their contrast is most pronounced during winter with 82 % positive temperature deviations (68 % negative ones) for EAWR+ (EAWR-). This linkage indicates that the West European teleconnection centre determines the temperature response at Mount Zugspitze (positive with an anticyclonic, negative with a cyclonic system).

EAWR is the only of the four analyzed teleconnection patterns with significant phase distinctions for precipitation during all seasons (yet least pronounced in summer). This is in general accordance to findings of Qian et al. (2000) who identified a partly similar pattern (so-called 'North-Sea Pattern') as the most important one for precipitation in Europe. Mostly the impact of EAWR+ on decreased precipitation is dominating (see Tab. 4), however, during winter this changes to a distinct preference for increased precipitation with EAWR-. Thus, in the cold season the efficiency of the cyclonic phase around the North Sea seems to be more pronounced than that of its anticyclonic counterpart.

7.4.2.4 Scandinavian Pattern (SCAND)

This pattern includes two opposing centres of variation above Scandinavia (anticyclonic system in the positive phase) and above the Iberian peninsula (Fig. 13). It has been identified in several studies (e. g. Wibig 1999; Quadrelli et al. 2001; Efthymiadis et al. 2007), but nevertheless, it has the lowest number of significant signals in Zugspitze temperature and precipitation (Tab. 5) among the teleconnection patterns discussed in this contribution. During spring, a distinct preference for below-average precipitation is indicated for SCAND+, but during summer some

Tab. 4: As Tab. 2 but for the East Atlantic West Russia Pattern (EAWR)

a)

Frequency	Temperature ↑	Temperature ↓	Precipitation ↑	Precipitation ↓
Winter EAWR+	82%	18%	50%	50%
Winter EAWR-	32%	68%	79%	21%
Spring EAWR+	73%	27%	21%	79%
Spring EAWR-	30%	70%	46%	54%
Summer EAWR+	55%	45%	39%	61%
Summer EAWR-	45%	55%	55%	45%
Autumn EAWR+	69%	31%	31%	69%
Autumn EAWR-	26%	74%	58%	42%

b)

Intensity	Temperature ↑	Temperature ↓	Precipitation ↑	Precipitation ↓
Winter EAWR+	1.17	-0.72	0.51	-0.81
Winter EAWR-	0.53	-0.92	0.44	-0.71
Spring EAWR+	0.91	-0.95	1.13	-0.85
Spring EAWR-	0.66	-0.71	1.16	-0.52
Summer EAWR+	0.91	-0.85	0.75	-0.76
Summer EAWR-	0.76	-1.06	1.10	-0.70
Autumn EAWR+	0.98	-0.97	0.55	-0.91
Autumn EAWR-	0.46	-1.10	0.95	-0.54

Tab. 5: As Tab. 2 but for the Scandinavian Pattern (SCAND)

a)

Frequency	Temperature ↑	Temperature ↓	Precipitation ↑	Precipitation ↓
Winter SCAND+	53%	47%	44%	56%
Winter SCAND-	64%	36%	59%	41%
Spring SCAND+	53%	47%	20%	80%
Spring SCAND-	58%	42%	54%	46%
Summer SCAND+	31%	69%	50%	50%
Summer SCAND-	69%	31%	30%	70%
Autumn SCAND+	58%	42%	27%	73%
Autumn SCAND-	50%	50%	42%	58%

b)

Intensity	Temperature ↑	Temperature ↓	Precipitation ↑	Precipitation ↓
Winter SCAND+	0.62	-0.73	0.48	-0.60
Winter SCAND-	1.01	-0.84	0.97	-0.62
Spring SCAND+	0.66	-0.92	0.37	-0.68
Spring SCAND-	0.86	-1.39	1.32	-0.81
Summer SCAND+	0.40	-0.86	0.94	-0.65
Summer SCAND-	0.90	-0.67	0.52	-0.68
Autumn SCAND+	0.85	-0.87	1.03	-0.72
Autumn SCAND-	0.79	-0.62	0.86	-0.68

changes in the relationships can be observed: now the negative phase is decisive but once more in favor of below-average precipitation (Tab. 5). This is due to a much more widespread southern centre of variation during summer (not shown in Fig. 13) including in particular the Alpine region. For SCAND- this means anticyclonic influence (reduced precipitation as well as increased temperatures), and for SCAND+ this implies cyclonic influence which, however, is clearly reflected only in reduced temperatures, whereas for precipitation no frequency distinction but only slightly greater amounts in the mean normalized anomalies for positive deviations (Tab. 5) can be observed. Generally, the SCAND pattern seems to be characterized by a high level of internal variability thus confining the frequency of associated climate anomalies.

7.5 Conclusions

Among the teleconnection patterns discussed in section 4.2, a very remote one has not been considered: the ENSO teleconnection. This may be justified in view of results by Efthymiadis et al. (2007) indicating that its impact on the climate of the Greater Alpine Region is generally weak and non-stationary (even in sign). Therefore our focus was on patterns well-known within the North-Atlantic European area, looking at conditions with pronounced positive or negative phases of these patterns (beyond one standard deviation from long-term mean values in the corresponding time coefficients). Remarkably, it was not the NAO among these patterns showing the strongest or most frequent impacts on temperature and precipitation anomalies at Mount Zugspitze, only in autumn and winter significant relationships could be confirmed, positive for temperature and winter precipitation (Atlantic influence with NAO+), but negative for autumn precipitation (i.e. increased frequencies of negative anomalies during NAO+ due to anticyclonic influence). EA and EAWR proved to have more often significant influence on seasonal anomalies at Mount Zugspitze. EA, some kind of a southward shifted NAO pattern, reveals positive relationships with temperature throughout the whole year, whereas Zugspitze precipitation is driven significantly only in summer and autumn (with EA+ favoring dry anomalies). EAWR, a dipole pattern with a zonal axis, impacts on Zugspitze conditions via its western centre around the North Sea, leading to positive relationships with temperature (except of summer) and seasonally varying influence on precipitation (mostly with EAWR+ favoring dry

anomalies, but in winter with EAWR- favoring wet anomalies). The lowest number of significant signals occurs with SCAND, a dipole pattern with meridional axis. During spring, SCAND+ favors dry anomalies, however, during summer the extended domain of the southern centre leads to inverted relationships (SCAND- favoring dry and warm anomalies, SCAND+ mainly cold anomalies).

Generally, the impact of characteristic modes of variability included in large-scale teleconnection patterns of the atmosphere, can be identified down to even local scales as shown for the example of Mount Zugspitze. Sometimes, however, these relationships may change their sign between different seasons or lose statistical significance. This indicates a high level of internal variability within one or both phases of the corresponding teleconnection patterns, for example with respect to position, extension or strength of the driving centres of variation which constitute the affected teleconnection pattern. Such 'within-type changes' are obviously quite common phenomena, as shown repeatedly in context of circulation dynamics (e. g. Jacobeit et al. 2001, 2003; Beck et al. 2007).

The other approach for identifying circulation-climate relationships presented in section 4.1 refers to basic circulation patterns (500 hPa level) which have been derived for months with temperature or precipitation anomalies (beyond one standard deviation from long-term mean values) at Mount Zugspitze. Large-scale trough patterns are primarily important for cold anomalies during both summer and winter, especially during the latter season since the influence of cold Russian high pressure systems does not extend up to mid-tropospheric levels. In contrast, various types of anticyclonic ridges induce warm anomalies, during summer mainly as ridges from the Azores towards southern Scandinavia (corresponding to the summer NAO+), during winter in terms of ridges with more meridional or zonal axis orientation. Additionally, during winter, an eastern Atlantic low pressure system (corresponding to the EA+ pattern) is linked with warm anomalies. During summer, this pattern is part of particular wave patterns which may be associated with both warm and cold anomalies depending on varying wave lengths and phase positions in context of pronounced within-type variability.

Basic circulation patterns for wet and dry anomalies have been presented for the transitional seasons. They include central low or high pressure systems and trough or ridge patterns towards Central Europe with clear-cut attribution to wet or dry anomalies, respectively. Furthermore, various wave patterns do occur with mixed anomaly attribution depending on varying amplitudes and axis positions.

Concerning results from both S-mode and T-mode analyses with respect to climate conditions at Mount Zugspitze, we may generally conclude that some modes or patterns of the large-scale atmospheric circulation include a definite link with local anomalies in temperature or precipitation on a monthly scale, whereas some other modes or patterns are characterized by an elevated level of internal variability leading to ambiguous impacts on local climate anomalies.

References

Appenzeller, C., T. F. Stocker and A. Schmittner (2000): Natural climate variability and climate change in the North-Atlantic European region: chance for surprise? Integrated Assessment 1, 301–306.

Auer I., R. Böhm, A. Jurkovic et al. (2007): HISTALP — historical instrumental climatological surface time series of the Greater Alpine Region. Int. J. Climatol. 27, 17–46.

Beck, C., J. Jacobeit and P. D. Jones (2007): Frequency and within-type variations of large scale circulation types and their effects on low-frequency climate variability in Central Europe since 1780. International Journal of Climatology 27, 473–491.

Climate Prediction Center (CPC): http://www.cpc.ncep.noaa.gov/data/teledoc/telecontents.shtml

Compagnucci, R. H., D. Araneo and P. O. Canziani (2001): Principal sequence pattern analysis: a new approach to classifying the evolution of atmospheric systems. Int. J. Climatol. 21, 197–217.

Compagnucci, R. H. and M. B. Richman (2008): Can principal component analysis provide atmospheric circulation or teleconnection patterns? Int. J. Climatol. 28, 703–726.

Dünkeloh, A. and J. Jacobeit (2003): Circulation dynamics of Mediterranean precipitation variability 1948–1998. Int. J. Climatol. 23, 1843–1866.

Efthymiadis, D., P. D. Jones, K. R. Briffa, R. Böhm and M. Maugeri (2007): Influence of large-scale atmospheric circulation on climate variability in the Greater Alpine Region of Europe. Journal of Geophysical Research 112, D12104, doi:10.1029/2006JD008021.

Folland, C.K, J. Knight, H.W. Linderholm, D. Fereday, S. Ineson and J.W. Hurrell (2009): The summer North Atlantic Oscillation: Past, Present, and Future. Journal of Climate 22, 1082–1103.

Jacobeit, J. (1992): Die großräumige Höhenströmung in der Hauptregenzeit feuchter und trockener Jahre über dem südamerikanischen Altiplano (Large-scale upper flow in the main rainy season of wet and dry years above the South-American Altiplano). Meteorologische Zeitschrift, N. F. 1, 276–284.

Jacobeit, J. (1993): Regionale Unterschiede im atmosphärischen Zirkulationsgeschehen bei globalen Klimaveränderungen (Regional differences of the atmospheric circulation under conditions of global climate change). Die Erde 124, 63–77.

Jacobeit, J. (2010): Classifications in Climate Research. Physics and Chemistry of the Earth 35, 411–421.

Jacobeit, J., C. Beck and A. Philipp (1998): Annual to Decadal Variability in Climate in Europe: Objectives and Results of the German Contribution to the European Climate Research Project ADVICE. Würzburger Geographische Manuskripte 43, 163 pp.

Jacobeit, J., P. D. Jones, T. Davies and C. Beck (2001): Circulation changes in Europe since the 1780s. In: Jones, P. D., A. E. Ogilvie, T. Davies and K. R. Briffa (Eds.): History and Climate: Memories of the Future. Kluwer Academic/Plenum Publishers, New York et al., pp. 79–100.

Jacobeit, J., H. Wanner, J. Luterbacher, C. Beck, A. Philipp, and K. Sturm (2003): Atmospheric circulation variability in the North-Atlantic-European area since the mid-seventeenth century. Climate Dynamics 20, 341–352.

Jacobeit, J., A. Philipp and M. Nonnenmacher (2006): Atmospheric circulation dynamics linked with prominent discharge events in Central Europe. Hydrological Sciences Journal 51, 946–965.

Jacobeit, J., A. Philipp, J. Rathmann and A. Walther (2009): European and North Atlantic daily to multidecadal climate variability: General Overview and Final Reports for the German Contribution to the European Climate Research Project EMULATE. Geographica Augustana 7, 65 pp.

Jolliffe, I.T (2002): Principal Component Analysis. Springer, New York et al., 487 pp.

Kalnay, E. et al. (1996): The NCEP/NCAR 40-year reanalysis project. Bull. Amer. Meteor. Soc. 77, 437–471.

Philipp, A., P. M. Della-Marta, J. Jacobeit, D. R. Fereday, P. D. Jones, A. Moberg, and H. Wanner (2007): Long term variability of daily North Atlantic-European pressure patterns since 1850 classified by simulated annealing clustering. Journal of Climate 20, 4065–4095.

Qian, B., J. Corte-Real and H. Xu (2000): Is the North Atlantic Oscillation the most important atmospheric pattern for precipitation in Europe? Journal of Geophysical Research 105 (D9), 11901–11910.

Quadrelli, R., M. Lazzeri, C. Cacciamani and S. Tibaldi (2001): Observed winter Alpine precipitation variability and links with large-scale circulation patterns. Climate Research 17, 275–284.

Richman, M. B. (1986): Rotation of principal components. Journal of Climatology 6, 293–335.

Schnur, R., G. Schmitz, N. Grieger and H. von Storch (1993): Normal modes of the atmosphere as estimated by principal oscillation patterns and derived from quasi-geostrophic theory. J. Atmos. Sci. 50, 2386–2400.

Von Storch, H. and F.W. Zwiers (1999): Statistical Analysis in Climate Research. Cambridge University Press, 484 pp.

Wibig, J. (1999): Precipitation in Europe in Relation to Circulation Patterns at the 500 hPa level. International Journal of Climatology 19, 253–269.